A MAGNETIC LEVITATOR BASED ON ROTATING SADDLE TRAP MECHANISM

B Shayak

Department of Theoretical and Applied Mechanics,
Sibley School of Mechanical and Aerospace Engineering,
Cornell University,
Ithaca – 14853,
New York, USA

sb2344@cornell.edu , shayak.2015@iitkalumni.org

*

Classification

PACS : 52.55.-s 45.40.-f

Keywords : Axisymmetric load field Octupolar trapping field Rotating saddle trap

Abstract

In this work I propose a mechanism for levitation and stable confinement of a heavy rotating body using electromagnetic interactions alone, with no position-dependent control. Support of load and vertical confinement are achieved through an axisymmetric magnetic field while lateral confinement is accomplished by a rotating octupolar field via the Brouwer saddle mechanism. The orientational degrees of freedom are stabilized through gyroscopic action. The design features multiple variable parameters, thus allowing considerable flexibility for scaling the system size and maximizing the basin of attraction of the stable state. The emphasis of this Article is on obtaining the equation of motion of the trap, and calculating its stability.

* * * * *

1 Introduction, design overview and operational principle

This Section is divided into four Subsections – the zeroth sets the background for this work, the first describes the mechanism itself and the second and third outline the physical principles behind the proposed mechanism.

1.0 Introduction

In 1842, SAMUEL EARNSHAW proved what is essentially a no-trapping theorem – that no configuration of charges or currents (or hypothetical magnetic monopoles) can be stably confined in space by any time-independent configuration of charges or currents in air or media with positive permittivity and permeability [1,2]. This one theorem forms the basis of the entire discipline of electromagnetic traps. Any kind of electromagnetic confinement must be achieved by aiming for the Achilles' heel, either by introducing time-dependence into the system or by using special materials with negative permeability. Perhaps the first instance of magnetic levitation was of the latter form, when in 1939, the German physicist WERNER BRAUNBECK levitated some diamagnetic graphite particles above a strong electromagnet. Sixty years later, SIR ANDRE GEIM, MARTIN SIMON and co-workers performed a highly innovative variant of this using a 16 Tesla magnetic field and a live frog as the levitator [3-5]. The ultimate manifestation of this effect would have been superconducting levitators, which are perfectly diamagnetic – when high T_c superconductivity was discovered in 1986 [6], it gave rise to tremendous expectations of practical levitators within the next few years [7]. Unfortunately, with the indefinite postponement of the discovery of room temperature superconductivity, the dreams of a working levitator built on these principles remained unfulfilled.

A different caveat in Earnshaw's theorem was targeted by WOLFGANG PAUL [8-10]. He bypassed the theorem by attacking the "time-independent" component; his trap features an electric field which is statically stable in two directions but unstable in the third, and then oscillates rapidly to stabilize the troublesome direction via the Kapitza pendulum mechanism. A second kind of particle trap called Penning trap was invented by HANS GEORG DEHMELT. Here, the electric and magnetic fields are static but the electrons themselves are driven along flowery trajectories through the interior of the trap [11,12]. The ingenuity of the design ensures that the electron is forever unstable to a perturbation along its path (there must be a lability direction as per Earnshaw's theorem) but the path is closed, and stable to deviations perpendicular to itself. (This concept has a parallel in nature – the gravitational attraction between stars and planets, which is also derived from a Laplacian potential, does not permit stable spatial confinement but has no objection against the stability of the solar system.) These two concepts ensured that the problem of electromagnetic trapping of microscopic particles was essentially solved. Although scope for improvement in design always remains, the basics are by now well established.

The story is very different if we look at electromagnetic trapping of extended objects rather than point particles. Although levitating trains and levitating motors are as desirable as their atomic counterparts from a practical point of view (the advantages of no contact friction and no contact stresses are obvious), a robust working design is yet to fructify. The existing levitators (called "magnetic bearings" in the mechanical and electrical engineering literature) use brute force to work round Earnshaw's theorem – they mount an array of electromagnets all connected to variable sources, continuously sense the position of the object and instantaneously excite the right set of electromagnets to counteract its immediate destabilization tendency [13]. Every dynamical system, howsoever unstable intrinsically, can always be stabilized through a sufficiently complex control arrangement, and this is the philosophy employed by these products. The inelegance of this solution is matched by its prohibitive cost, complexity and lack of reliability – as of today, Maglev trains carry passengers on exactly 59 km of track worldwide and magnetically levitated rotors occupy a similarly insignificant position in technology and industry.

The concepts of Paul and Penning traps are not directly generalizable to macroscopic systems – in the former case, the load cannot be supported by a time-varying field while in the latter case, a rigid body cannot be guided along a complicated trajectory. Moreover, the practical absence of electric charges on a macro scale compel such levitator designs to be based on magnets alone. The only design which achieves control-free magnetic levitation and stabilization of a macroscopic object is the toy called "Levitron", invented by ROY HARRIGAN and BILL HONES. This is a magnetic dipole in the shape of a top which floats above a magnetic block. The principles underlying this somewhat serendipitous invention were first explained by SIR MICHAEL BERRY [14]; he came up with a lovely explanation of how the spin of the top couples adiabatically to the magnetic field of the base, and how the stability is strengthened by an additional coupling between the magnetic field and the top's precession. In the rest of this Article, I will refer to the Levitron as the Harrigan-Hones-Berry or HHB confinement mechanism. Amazing as this

mechanism is, with a dc magnetic field achieving trapping and with the subtle underlying physics connecting to various aspects of quantum theory [15-17], it has not proved practically realistic due to the light weight of the rotor, the smallness of the basin of attraction of the stable state and the absence of external parameters which can be tuned to scale the system size or enhance its stability. Twenty years after its invention, the HHB mechanism still powers only a fascinating toy and nothing of greater import.

In this work I will propose a novel design for an electromagnetic rigid body trap. Like the HHB mechanism, it uses no active control but the manner of achieving confinement is closer in spirit to that of Paul trap. This enables the system size to be scaled as per the application requirements and allows for the introduction of several design parameters which can be optimized for maximal stability. The trap has a flat geometry so the design is compact, and the lift and stability are completely decoupled from the torque output of the driving motor. I will now present the drawing and description of the proposed apparatus.

1.1 Description of the apparatus

In this Subsection I will describe the design of the proposed trap with no justification or calculation. A diagram of the device is shown in Fig. 1.

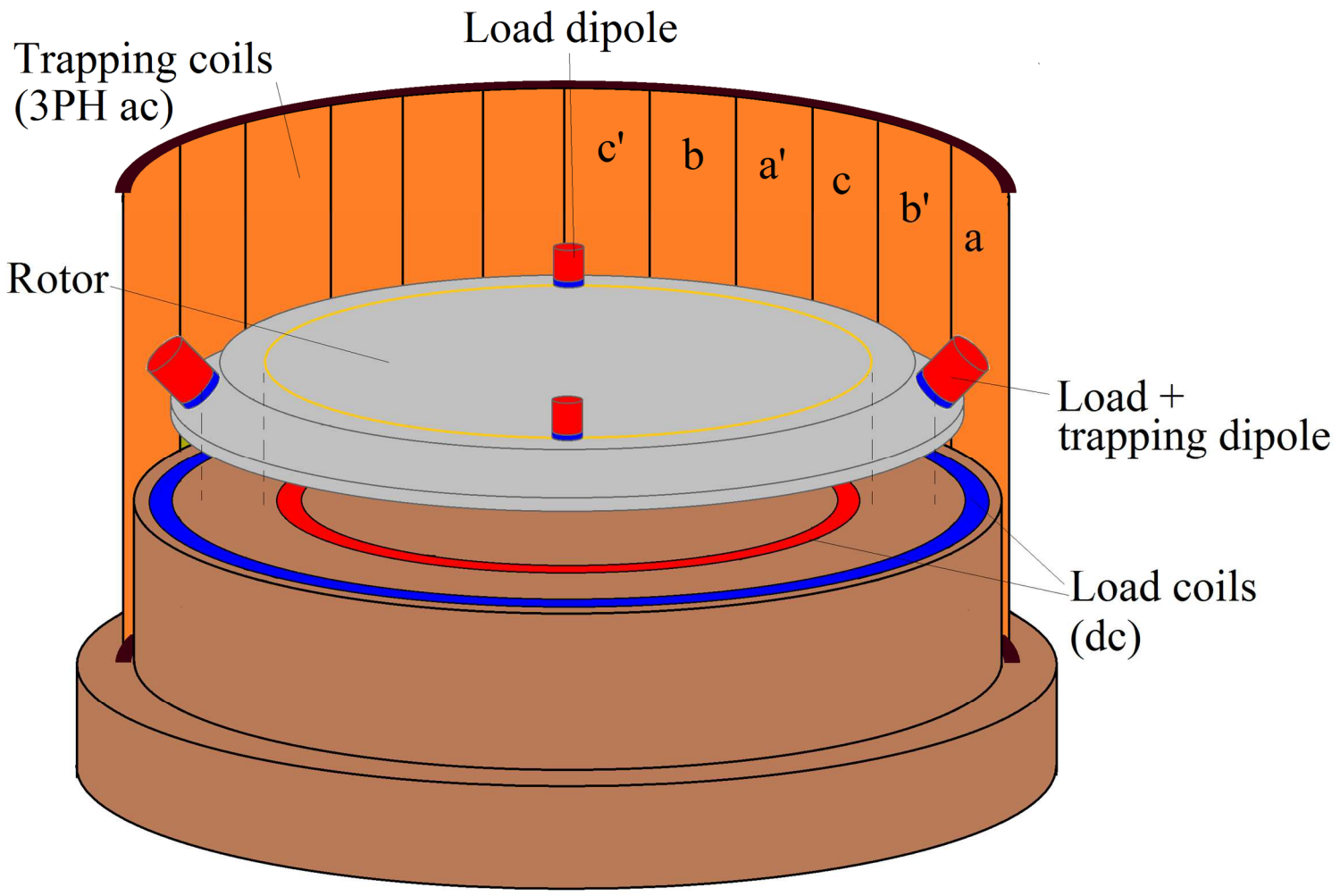

Figure 1 : *Schematic representation of the trap. For the dipoles, red denotes North and blue South. The load dipoles are mounted vertically, pointing upwards. The two inclined dipoles serve both load and trapping function. Here they point upwards and outwards; they can also be made to point inwards by turning the rotor upside down and flipping all the dipoles (which compromises Figure clarity). The mounting radii of the load and trapping dipoles are shown as grossly different; that too is for clarity only. The red load coil carries current counter-clockwise (CCW) while the blue one carries current clockwise (CW) when viewed from the top. The three-phase octupolar winding encloses the apparatus completely; half of it has been excised to reveal what lies inside. The phases are labelled as per standard electrical engineering convention [18] and have no relation to the mechanical* a,b,c *axes I will use in Subsection 2.1 onwards. The driving motor is not shown.*

The object to be confined, hereafter referred to as the "rotor" because it rotates, is circular with a vertical axis of symmetry and consists of four magnetic dipoles ("load dipoles") mounted at a fixed radius, equally spaced in the circumferential direction and pointing vertically upwards, and two more dipoles ("trapping dipoles"), again at equal radius and equally spaced, mounted in the plane of symmetry. The signs on these dipoles – whether they point inwards or outwards – should be determined from the system specifics. The load coils are a pair of circular wires carrying current in opposite directions – counterclockwise (CCW) on the inner wire and clockwise (CW) on the outer. These two wires are concentric and coaxial with the default position of the rotor; the radius of mounting of the dipoles is chosen halfway between those of the inner and outer wires. The trapping coils consist of a standard cylindrical three-phase eight-pole winding surrounding the rotor and the load coils; these must be coaxial with the rotor and the load coils and are long compared to the radius so that the field is essentially two-dimensional octupolar. They are excited with ac from a variable-voltage variable-frequency (VVVF) or equivalent inverter [18] so that the octupolar field can be adjusted to any given strength and rotated at any given speed. The mass of the rotor is arranged in a flat manner so that the axial moment of inertia can be maximized. The motor powering the rotor may be either induction or permanent magnet synchronous, which are both contactless. Calculations show that in the two-dimensional limit (height>>radius), a rotor of polarity $2m$ feels a lateral force when displaced from the centre of the stator magnetic field of polarity $2n$ if and only if $n>m$. This implies that motors (where $m=n$ by definition) with predominantly fundamental harmonics in the windings will undergo very small lateral forces in response to rotor perturbations normal to the axis. Hence the motor will neither augment not detract the stability of the overall system and I will ignore it completely in what follows.

Words and Figure complete, we can now start the analysis of the trap.

1.2 The Brouwer saddle mechanism

A century ago, the Dutch mathematician BERTUS BROUWER proved a result [19] which was 50 years ahead of its time and does not fail to surprise even today. This was that if a particle is placed at the centre of a saddle potential and the saddle rotated, then there are regions in the saddle strength vs. rotational speed parameter space where the particle is actually stable. A detailed analysis of this system, in terms which are understandable to the modern dynamicist, has been performed by OLEG KIRILLOV [20,21]. Applications of the result to particle traps may be found in References [22-24]. Since this mechanism will form the backbone of the proposed rigid body trap, I will now present a simplified but sufficiently accurate treatment of its dynamics.

Let the laboratory frame be characterized by the coordinates x,y,z and a second frame, rotating relative to the lab about the z-axis, by the coordinates x',y',z'. Let the angle of rotation be θ so that $[x';\, y';\, z'] = \mathbf{Z}(\theta)[x;\, y;\, z]$, where the semi-colon notation, alla Matlab, indicates a new row. In the rotating frame, the saddle potential is $V(x',y') = A\left(x'^2 - y'^2\right)$ where A is the strength (the longitudinal and transverse strengths are chosen equal because that is the way things will work out in the trap). Doing the conversion to x,y,z basis yields the potential in the lab frame; if the saddle rotates CW at a constant rate $\omega/2$ relative to the lab, we can set $\theta=-\omega t/2$ into this expression and then write $\mathbf{F} = -\nabla\mathbf{V}$ to get the equation of motion

$$\ddot{x} = 2A\left(-x\cos\omega t + y\sin\omega t\right) \quad , \tag{1.1a}$$

$$\ddot{y} = 2A\left(x\sin\omega t + y\cos\omega t\right) \quad . \tag{1.1b}$$

Following LANDAU's treatment of the Kapitza pendulum we do a direct partition of motion into slow and fast, writing $x=x_s+x_f$ and $y=y_s+y_f$ where the 's' components vary slowly and the 'f' components vary rapidly, oscillating at frequency ω; solving for the fast components and averaging over them gives the slow equations

$$\ddot{x}_s = -\frac{4A}{\omega^2}x_s \quad , \tag{1.2a}$$

$$\ddot{y}_s = -\frac{4A}{\omega^2}y_s \quad , \tag{1.2b}$$

which clearly describes a spring in both directions.

A physical explanation for this counter-intuitive phenomenon is as follows : suppose the particle is located at some positive x-coordinate and is stationary or nearly stationary. Then, consider one particular instant of time when the saddle is downhill in x; the particle will feel a rightwards force and proceed further in x. But since the potential is

rotating, a short while later the saddle will become uphill in x and this will now exert a leftward force on the particle. The key step is that at this new instant the particle is *further* from the origin than it was earlier; since the magnitude of the force is proportional to the displacement, this leftward force will be stronger than the earlier rightward force and the two forces will average out to a *negative* resultant that is proportional to the displacement. This is exactly the conclusion which is seen quantitatively in (1.2).

1.3 The Physics behind the trap

In this Subsection, I will outline the motivation behind the design and touch upon the physics which makes the trap work. The treatment will be extremely brief since the details are in Reference [25]; the primary purpose of this Article is to elucidate the mathematical development behind the almost entirely qualitative treatment of the Letter. Since the rotor is going to levitate, the rotor electromagnetic elements must be independent of space and time with respect to its own frame. Magnetic dipoles rather than battery-fed windings are the natural choice because they abound in nature and in factories; moreover, permanent magnet dipoles offer great strength at small size and mass. They are also size-scalable; if n dipoles support and confine a rotor of mass M, $2n$ dipoles will (at least in general – see below) work for a rotor of mass $2M$.

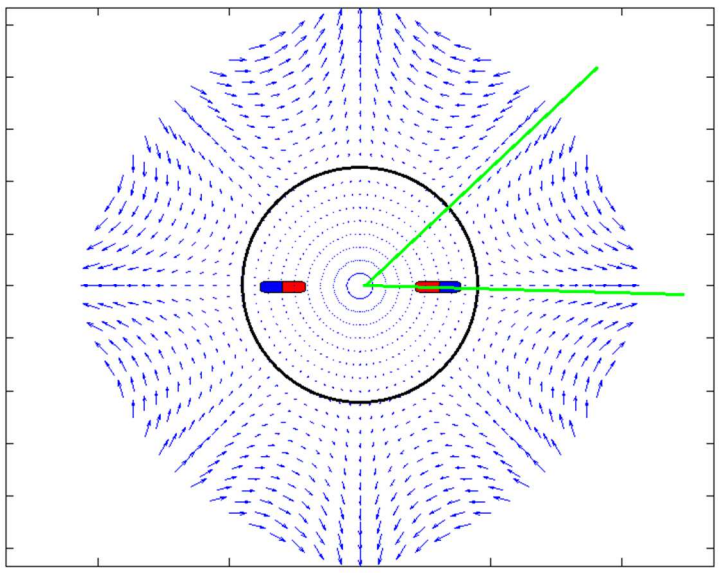

Figure 2 : *The octupolar trapping field with the rotor inside it. In the present alignment, the rotor is stable to a displacement along the horizontal green line and unstable to a displacement perpendicular to it. When the rotor orientation becomes along the green line at 45^o angle, the parallel and perpendicular stabilities interchange. As the rotor rotates, this amounts to an effective rotating saddle potential, which lies at the heart of the proposed mechanism.*

In summary, the lift force is generated by interaction of the load dipoles with the load field. The default 'cruising altitude' z_0 is chosen in such a manner that the rotor is statically stable in z. This of course generates a static instability in x and y. The function of the trapping field and dipoles is to counter this instability. As the rotor rotates through the octupolar field (Fig. 2), it is sometimes stable to a perturbation along the line of the trapping dipoles and sometimes stable to displacement in a perpendicular direction. This is equivalent to the Brouwer saddle. The effective spring arising from the Brouwer saddle overcomes the instability from the load field and dipoles. Stabilization of rotational dynamics is achieved via gyroscopy. Also, the trapping field must be rotated at some finite rate relative to the laboratory so that the nutational torque arising from its interaction with the trapping dipoles averages out to zero in time. We now go on to the mathematical expression of these concepts.

2 Linearized equations of motion

In this Section I will obtain the equation of motion of the rotor upto first order in translational and orientational perturbations about the default operating state. The first Subsection sets up the system and the next two Subsections calculate the effect of the load configuration followed by that of the trapping configuration.

2.1 Setup and variable definitions

Any description of the complete motion of a rigid body must feature six configuration variables – three position and three orientation. In this problem, none of the variables is trivial or redundant and so we must develop six second order equations of motion. The translational variables are the x, y and z coordinates of the rotor centre of mass (CM)

relative to their reference positions, which are 0, 0 and z_0 measured from the geometric centre of the ground-fixed load coils; we call these perturbations x_{CM}, y_{CM} and z_{CM}. For analysis of rotational dynamics, we assume that the rotor is symmetric with axial moment of inertia I_c and the two transverse moments equal to some value I. To characterize the orientation, we fix the origin at the rotor CM and use Euler angles in Euler or gyroscope convention. Starting from the reference basis x,y,z the first rotation (precession) through φ about z-axis takes us to x',y',z', the next rotation (nutation) through θ about x'-axis takes us to a,b,c, and the final rotation (spin) through ψ about c-axis takes us to the body-aligned frame d,q,o. We let the n^{th} rotor dipole (either load or trapping) be located at a point whose position vector from the rotor CM in the d,q,o frame makes an angle β_n with the d-axis; thus this vector can be written as $r_0 \cos\beta_n \hat{\mathbf{d}} + r_0 \sin\beta_n \hat{\mathbf{q}}$, where r_0 is the radius of the dipole ring. The orientation of all load dipoles is along the o-axis while the n^{th} trapping dipole points along the negative of the position vector to its location. Let the strength of each load dipole be m_1 and that of each trapping dipole be m_2.

The rotation matrices from x,y,z to a,b,c and d,q,o bases are

$$\mathbf{R}_{xyz}^{abc} = \mathbf{X}(\theta)\mathbf{Z}(\varphi) = \begin{bmatrix} \cos\varphi & \sin\varphi & 0 \\ -\sin\varphi\cos\theta & \cos\varphi\cos\theta & \sin\theta \\ \sin\varphi\sin\theta & -\cos\varphi\sin\theta & \cos\theta \end{bmatrix} \quad , \tag{2.1a}$$

$$\mathbf{R}_{xyz}^{dqo} = \mathbf{Z}(\psi)\mathbf{X}(\theta)\mathbf{Z}(\varphi) = \begin{bmatrix} \cos\varphi\cos\psi - \sin\varphi\cos\theta\sin\psi & \sin\varphi\cos\psi + \cos\varphi\cos\theta\sin\psi & \sin\theta\sin\psi \\ -\cos\varphi\sin\psi - \sin\varphi\cos\theta\cos\psi & -\sin\varphi\sin\psi + \cos\varphi\cos\theta\cos\psi & \sin\theta\cos\psi \\ \sin\varphi\sin\theta & -\cos\varphi\sin\theta & \cos\theta \end{bmatrix} \quad , \tag{2.1b}$$

and these can be used to obtain the positions and orientations of all the dipoles. The electromagnetic force and torque on each dipole can then be obtained as

$$\mathbf{F} = \sum_{\text{all dipoles } n} (\mathbf{m}_n \cdot \nabla)\mathbf{B}_n \quad , \tag{2.2a}$$

$$\mathbf{T} = \sum_{\text{all dipoles } n} (\mathbf{r}_n \times \mathbf{F}_n + \mathbf{m}_n \times \mathbf{B}_n) \quad , \tag{2.2b}$$

where the summations run over the load as well as the trapping dipoles and $\mathbf{B}_n$ denotes the magnetic field at the location of dipole n arising from the load as well as the trapping coils (the contributions from the other rotor dipoles to this field can be neglected since we know that the rotor exerts no force or torque on itself). Note that in (2.2b), $\mathbf{r}_n$ denotes the vector from the rotor CM to the n^{th} dipole.

The translational equations of motion are straightforward :

$$\ddot{x}_{CM} = F_x / M \quad , \tag{2.3a}$$

$$\ddot{y}_{CM} = F_y / M \quad , \tag{2.3b}$$

$$\ddot{z}_{CM} = F_z / M - g \quad , \tag{2.3c}$$

where M is the rotor mass, while the rotational equations can be obtained by evaluating the material derivative of angular momentum in the a,b,c basis,

$$I\ddot{\theta} + I_c(\ddot{\psi} + \dot{\varphi}\cos\theta)\dot{\varphi}\sin\theta - I\dot{\varphi}^2\cos\theta\sin\theta = T_a \quad , \tag{2.4a}$$

$$I\ddot{\varphi}\sin\theta + (2I - I_c)\dot{\varphi}\dot{\theta}\cos\theta - I_c\dot{\theta}\dot{\psi} = T_b \quad , \tag{2.4b}$$

$$I_c(\ddot{\psi} + \ddot{\varphi}\cos\theta + \dot{\varphi}\dot{\theta}\sin\theta) = T_c \quad . \tag{2.4c}$$

These are the equations of motion of the rotor.

For analytical progress, we will now make a simplification. Due to the extreme difficulty of a full analytical characterization of the magnetic field, we shall not attempt to obtain nonlinear equations. Rather, having satisfied ourselves through symmetry arguments or easy calculations that the reference configuration is a fixed point of the system (2.1-4), we will restrict x_{CM}, y_{CM}, z_{CM} and θ to small values and calculate forces and torques only upto linear order in these variables. We will then use these linearized forms to perform a stability analysis of the fixed point. This method of ad hoc linearization, although not as theoretically satisfying as the derivation of full nonlinear equations, is completely adequate from a practical point of view since the reference configuration is the only desirable operating condition of the system and must be linearly stable for the trap to be effective.

For the linearized analysis we will require the first spatial derivatives of force and torque, evaluated at the reference point. Since force features the gradient of **B**, this means that we will need every possible second spatial derivative of every component of **B**, evaluated at the reference position. Once this is done, we can expand the forces and torques in Taylor serieses and plug in the derivatives to obtain the linearized equations. This is the general scheme which I will be following repeatedly in the below Subsections.

2.2 Forces and torques from the load field

The load coils consist, at least in our model, of a pair of concentric circular coils carrying current. The magnetic field due to a circular coil is exactly solvable in theory [2]; unfortunately the Legendre series expansions are in powers of the radius ratio and convergence is very poor near the coil itself. Hence we use the Biot Savart integral instead, in cylindrical coordinates ρ,γ,z with the origin at the coil centre. We consider a single coil of radius r, carrying current i and mounted in a linear medium of permeability μ. Clearly, B_γ must be exactly zero while the other two components are given by

$$B_\rho = \frac{\mu i}{4\pi}\int_0^{2\pi} \frac{rz\cos\gamma'\,\mathrm{d}\gamma'}{\left(\rho^2 - 2r\rho\cos\gamma' + r^2 + z^2\right)^{3/2}} \quad , \tag{2.5a}$$

$$B_z = \frac{\mu i}{4\pi}\int_0^{2\pi} \frac{\left(r^2 - r\rho\cos\gamma'\right)\mathrm{d}\gamma'}{\left(\rho^2 - 2r\rho\cos\gamma' + r^2 + z^2\right)^{3/2}} \quad . \tag{2.5b}$$

These integrals are not doable exactly, so we first separate the denominator into two parts, one containing the ρ,γ dependence and the other being the z term. We then expand it in a Taylor series

$$\frac{1}{\left(\rho^2 - 2r\rho\cos\gamma' + r^2 + z^2\right)^{3/2}} = \frac{1}{\left(\rho^2 - 2r\rho\cos\gamma' + r^2\right)^{3/2}}\left[1 - \frac{3}{2}\frac{z^2}{\rho^2 - 2r\rho\cos\gamma' + r^2} + \frac{15}{8}\frac{z^4}{\left(\rho^2 - 2r\rho\cos\gamma' + r^2\right)^2} + \ldots\ldots\right] \quad . \tag{2.6}$$

Now we see that if ρ is close to r, then the denominator in each term is sharply peaked near $\gamma'=0$; this region has the largest contribution when the integration over γ' is carried out. Letting $\varepsilon=(\rho-r)/r$, considering the region $-\varepsilon<\theta<\varepsilon$ alone, the integral in each term acquires a contribution of $\varepsilon^{1-2\alpha}$, where α is the exponent of $\rho^2 - 2r\rho\cos\gamma' + r^2$ in that term. Since this is large, it dominates over the contribution arising from the other regions. Accordingly, B_ρ might be written as

$$B_\rho = iz\left[\frac{A_1}{(\rho - r)^2} - \frac{A_2 z^2}{(\rho - r)^4} + \ldots\ldots\right] \quad , \tag{2.7}$$

where A_1 and A_2 are positive, $O(1)$ constants. Similarly B_z might be written as

$$B_z = i\left[-\frac{A_3}{\rho - r} + \frac{A_4 z^2}{(\rho - r)^3} - \frac{A_5 z^4}{(\rho - r)^5} + \ldots\ldots\right] \quad , \tag{2.8}$$

where the A's are again positive and $O(1)$.

Although I have to admit that the derivation of these serieses is less than rigorous, they do bring out several features which are supported by numerical work. For example, B_ρ is zero at $z=0$ and increases as one goes upwards, before going over to a decreasing trend. B_z is positive if $\rho<r$ and negative if $\rho>r$ (we recall that this coil carries current CCW); focusing on the latter region, as we move upwards, the field strength decreases rapidly at first but more slowly later on. When there are two coils of radius r_1 and r_2 carrying currents $+i$ and $-i$ respectively, then at the point midway between the coils i.e. at $\rho=(r_1+r_2)/2$, B_ρ becomes exactly zero for all z.

On the basis of these observations, I will now write the magnetic field which will actually be used for the calculations. Since the analysis is linearized, I will require B_ρ and B_z only in a small cylindrical annulus centred around $\rho=r_0$ and $z=z_0$. I will assume that the following are true :

- $B_z\big|_{r0,z0} = -B_0$, where B_0 is some positive quantity
- $\partial B_z / \partial z\big|_{r0,z0} = C_1$, where C_1 is positive (it supports the rotor weight)
- $\left.\dfrac{\partial^2 B_z}{\partial z^2}\right|_{r0,z0} = -C_2$, where C_2 is positive (this is essential for static z-stability of the rotor)
- $B_\rho\big|_{r0,z} = 0$ for all z.

These four assumptions, together with the zero conditions on the divergence and curl of **B**, and all derivatives thereof, determine **B** in the annulus as

$$B_\rho = 0 - C_1(\rho - r_0) + C_2(\rho - r_0)(z - z_0) + \ldots\ldots \quad , \tag{2.9a}$$

$$B_z = -B_0 + C_1(z - z_0) + \frac{1}{2}C_2\left[(\rho - r_0)^2 - (z - z_0)^2\right] + \ldots\ldots \quad . \tag{2.9b}$$

Although these expressions are approximate, they do not miss out on anything important. The tricky dynamics of the system all arise from Earnshaw's theorem which in turn comes from the conditions on the divergence and curl of **B**; since I have explicitly ensured the vanishing of these in (2.9), the simplifications do not throw away any potential sources of real trouble.

Given the field, we can now write the force terms. We have

$$F_i = \sum_{\text{all dipoles}} \left[\sum_j m_j \frac{\partial B_i}{\partial x_j} \right] \quad , \tag{2.10}$$

where i and j are indices and not dipole numbers. Then,

$$F_i = \sum_{\text{all dipoles}} \left[\sum_j \left(m_{j,\text{def}} \left.\frac{\partial B_i}{\partial x_j}\right|_{\text{def}} \right) + \sum_j \left(m_{j,\text{pert}} \left.\frac{\partial B_i}{\partial x_j}\right|_{\text{def}} \right) + \sum_{j,k} \left(m_{j,\text{def}} \left.\frac{\partial^2 B_i}{\partial x_j \partial x_k}\right|_{\text{def}} \Delta x_k \right) \right] \quad , \tag{2.11}$$

where 'def' stands for default and indicates inclusion of only large terms while 'pert' stands for perturbation and indicates inclusion of linear terms in small quantities. We can easily verify that the sums of all the 'default' terms in the force is zero (except in the z-direction where it is Mg), leaving us with quantities proportional to the various perturbations.

The location of dipole n relative to the default CM position $(0,0,z_0)$, can be written from the linearized (2.1) as

$$\mathbf{r}_n = \left[r_0 \cos(\varphi + \psi + \beta_n) + x_{CM} \right]\hat{\mathbf{x}} + \left[r_0 \sin(\varphi + \psi + \beta_n) + y_{CM} \right]\hat{\mathbf{y}} + \left[r_0\theta \sin(\psi + \beta_n) + z_{CM} \right]\hat{\mathbf{z}} \quad . \tag{2.12}$$

Similarly the n^{th} dipole moment vector is

$$\begin{aligned}\mathbf{m}_n = &\left[-m_2 \cos(\varphi + \psi + \beta_n) + m_1\theta \sin\varphi \right]\hat{\mathbf{x}} + \left[-m_2 \sin(\varphi + \psi + \beta_n) - m_1\theta \cos\varphi \right]\hat{\mathbf{y}} + \\ &\left[-m_2\theta \sin(\psi + \beta_n) + m_1 \right]\hat{\mathbf{z}}\end{aligned} \quad . \tag{2.13}$$

The default and perturbation terms can be clearly seen in these expressions.

Similar to (2.11) the torque can be written as

$$
\begin{aligned}
T_i &= \sum_{\text{all dipoles}} \left[r_j F_k - r_k F_j + m_j B_k - m_k B_j \right] \\
&= \sum_{\text{all dipoles}} \left[r_j \sum_l m_l \frac{\partial B_k}{\partial x_l} - r_k \sum_l m_l \frac{\partial B_j}{\partial x_l} + m_j B_k - m_k B_j \right] \\
&= \sum_{\text{all dipoles}} \left[\begin{array}{l}
r_{j,\text{def}} \left(\sum_{l,p} \left(m_{l,\text{def}} \left. \frac{\partial^2 B_k}{\partial x_l \partial x_p} \right|_{\text{def}} \Delta x_p \right) + \sum_l \left(m_{l,\text{pert}} \left. \frac{\partial B_k}{\partial x_l} \right|_{\text{def}} \right) \right) + r_{j,\text{pert}} \sum_l m_l \left. \frac{\partial B_k}{\partial x_l} \right|_{\text{def}} - \\
r_{k,\text{def}} \left(\sum_{l,p} \left(m_{l,\text{def}} \left. \frac{\partial^2 B_j}{\partial x_l \partial x_p} \right|_{\text{def}} \Delta x_p \right) + \sum_l \left(m_{l,\text{pert}} \left. \frac{\partial B_j}{\partial x_l} \right|_{\text{def}} \right) \right) - r_{k,\text{pert}} \sum_l m_l \left. \frac{\partial B_j}{\partial x_l} \right|_{\text{def}} + \\
m_{j,\text{def}} \sum_l \left. \frac{\partial B_k}{\partial x_l} \right|_{\text{def}} \Delta x_l + m_{j,\text{pert}} B_{k,\text{def}} - m_{k,\text{def}} \sum_l \left. \frac{\partial B_j}{\partial x_l} \right|_{\text{def}} \Delta x_l + m_{k,\text{pert}} B_{j,\text{def}}
\end{array} \right],
\end{aligned}
\tag{2.14}
$$

where **r** now denotes the position vector from the rotor CM to the dipoles and the sum over dipoles includes both load and trapping. Once again, we can verify quite easily that all default terms add up to zero, so I have included only perturbation terms in (2.14).

While doing the trigonometry in the above calculations, the most important observation is that a lot of second harmonics in $\varphi+\psi+\beta_n$ arise during the process. Such fluctuating forces and torques are undesirable, and can be cancelled off if the number of load and trapping dipoles is 4, or a multiple thereof. Hence I have shown 4 load dipoles in the original design, Fig. 1. Four trapping dipoles would have been ideal too; unfortunately, we will see in the next Subsection that this will also nullify the Brouwer saddle effect, and will amount to throwing the baby out with the bathwater. Hence we must stick to 2 trapping dipoles and live with the second harmonics.

Starting from (2.11), tedious but straightforward algebraic manipulations give us :

$$
F_x = \frac{C_1 m_2}{r_0} \left[x_{CM} \left\{ 1 - \cos 2(\varphi+\psi) \right\} + y_{CM} \left\{ \frac{1}{2} \sin 4(\varphi+\psi) \right\} \right] - 2C_1 m_1 \theta \sin\varphi + C_2 m_1 x_{CM} \quad , \tag{2.15a}
$$

$$
F_y = \frac{C_1 m_2}{r_0} \left[x_{CM} \left\{ -\frac{1}{2} \sin 4(\varphi+\psi) \right\} + y_{CM} \left\{ 1 - \cos 2(\varphi+\psi) \right\} \right] + 2C_1 m_1 \theta \cos\varphi + C_2 m_1 y_{CM} \quad , \tag{2.15b}
$$

$$
F_z = -2C_2 m_1 z_{CM} \quad . \tag{2.15c}
$$

Likewise, more algebra converts (2.14) into :

$$
T_x = 2r_0 m_2 \left[-\frac{C_2}{2} x_{CM} \sin 2(\varphi+\psi) + C_2 y_{CM} \sin^2(\varphi+\psi) - 3C_1 \theta \sin\psi \sin(\varphi+\psi) \right] + 4m_1 B_0 \theta \cos\varphi + 2C_1 m_1 y_{CM} \, , \tag{2.16a}
$$

$$
T_y = 2r_0 m_2 \left[C_2 x_{CM} \cos^2(\varphi+\psi) + \frac{C_2}{2} y_{CM} \sin 2(\varphi+\psi) + C_1 \theta \sin\psi \cos(\varphi+\psi) \right] - 4m_1 B_0 \theta \sin\varphi - 2C_1 m_1 x_{CM} \quad . \tag{2.16b}
$$

The role of T_z is to affect the rotation speed of the rotor. Since that is (*a*) fast to begin with, (*b*) physically bound to remain constant on the long term, and (*c*) controlled externally by the user depending on the application, T_z is not a quantity of interest.

These are the expressions for force and torque on the rotor on account of the load field alone. In the next Subsection I will calculate the equivalents for the trapping field, and after that put them all together to draw conclusions regarding the system stability.

2.3 Forces and torques from the trapping field

The trapping coils consist of a three-phase eight-pole winding of radius R carrying surface current of the form $\mathbf{K} = (K_0 \cos 4\gamma)\hat{\mathbf{z}}$. If we assume the current to extend infinitely in z (an assumption which is good if the height of the windings is large compared to the radius), then the calculation of its magnetic field is a standard exercise in electromagnetism :

$$
\mathbf{B} = \frac{\mu K_0 \rho^3}{2R^3} \left[(\cos 4\gamma)\hat{\boldsymbol{\rho}} - (\sin 4\gamma)\hat{\boldsymbol{\gamma}} \right] \quad . \tag{2.17}
$$

Of course, there is no B_z and no dependence of **B** on z because of the infinite extent there. In Cartesian coordinates, which is what we want for (2.11) and (2.14),

$$\mathbf{B} = \frac{\mu K_0}{2R^3}\left[\left(x^3 - 3xy^2\right)\hat{\mathbf{x}} + \left(-3x^2 y + y^3\right)\hat{\mathbf{y}}\right] \quad . \tag{2.18}$$

Due to the rotation of the three-phase current however, this expression will in general be valid not in the x,y basis but in a new basis x_r,y_r which makes an angle $\zeta(t)$ with the x,y basis. Thus **B** will actually be (2.18) with x,y replaced by x_r,y_r, and the conversion between the bases will be given by

$$\begin{bmatrix} x_r \\ y_r \end{bmatrix} = \begin{bmatrix} \cos\zeta & \sin\zeta \\ -\sin\zeta & \cos\zeta \end{bmatrix} \begin{bmatrix} x \\ y \end{bmatrix} \quad , \tag{2.19a}$$

$$\begin{bmatrix} B_x \\ B_y \end{bmatrix} = \begin{bmatrix} \cos\zeta & -\sin\zeta \\ \sin\zeta & \cos\zeta \end{bmatrix} \begin{bmatrix} B_{xr} \\ B_{yr} \end{bmatrix} \quad . \tag{2.19b}$$

The calculation of the first and second derivatives of this appears difficult but a trick simplifies the process.

We recognize that all the derivatives of the un-rotated **B** (2.18) are linear or quadratic polynomials in x and y. Moreover, all these need to be evaluated at the default position, which is $x = r_0\cos\left(\varphi+\psi+\beta_n\right)$ and $y = r_0\sin\left(\varphi+\psi+\beta_n\right)$. Now, if the field is rotated by angle ζ, then surely things will be the same if we assume the field to be stationary and subtract off an angle ζ from the argument of the trigonometric functions in x and y. Well, almost but not quite. The catch is that because of the four-fold symmetry of the octupolar field (Fig. 2), if the axes x_r,y_r perform one rotation relative to x,y then the field actually performs *four* rotations relative to the default configuration. Hence, it is actually four ζ's which needs to be subtracted from the argument and not just one ζ. Quick check : if ζ=90° then the field and all its derivatives are identical to when ζ=0, consistent with the factor of 4.

Some manipulation takes us to the next point of conceptual subtlety. After some trigonometry we arrive at the following expression for F_x :

$$F_x = \frac{3\mu K_0 r_0 m_2}{R^3} \sum_{\text{all dipoles } n}\left[x_{CM}\left\{-\cos 2\left(\varphi+\psi+\beta_n-4\zeta\right)\right\} + y_{CM}\left\{\sin 2\left(\varphi+\psi+\beta_n-4\zeta\right)\right\}\right] \quad . \tag{2.20}$$

If we now have four trapping dipoles here i.e. β_n=0, 90°, 180° and 270°, then the coefficients of x_{CM} and y_{CM} both cancel in pairs, and a potential Brouwer saddle turns into a meaningless triviality. This conclusion can also be motivated by studying Fig. 2, imagining four trapping dipoles instead of two and using the zero divergence and curl of **B**. In the general case we can safely say that if the polarity of the trapping field is $2n$, the number of trapping dipoles can NOT be a multiple of n. On the other hand, since the load dipoles are not involved in trapping, there is no need to impose this restriction on their number, and we should choose it so as to cancel or minimize the amplitudes of near harmonics.

The rest now is again tedious algebra,

$$F_x = \frac{6\mu K_0 r_0 m_2}{R^3}\left[-x_{CM}\cos 2\left(\varphi+\psi-4\zeta\right) + y_{CM}\sin 2\left(\varphi+\psi-4\zeta\right)\right] \quad , \tag{2.21a}$$

$$F_y = \frac{6\mu K_0 r_0 m_2}{R^3}\left[x_{CM}\sin 2\left(\varphi+\psi-4\zeta\right) + y_{CM}\cos 2\left(\varphi+\psi-4\zeta\right)\right] \quad . \tag{2.21b}$$

F_z is identically zero since the trapping field is independent of z.

Manipulations involving (2.14) yield

$$\begin{aligned} T_x = {} & \frac{3\mu K_0 r_0^3 m_2}{R^3}\theta\sin\psi\left[\cos\left(\varphi+\psi\right)\sin 2\left(\varphi+\psi-4\zeta\right) - \sin\left(\varphi+\psi\right)\cos 2\left(\varphi+\psi-4\zeta\right)\right] - \\ & \frac{\mu K_0 r_0^3 m_2}{R^3}\theta\sin\psi\sin 3\left(\varphi+\psi-4\zeta\right) \end{aligned} \quad , \tag{2.22a}$$

$$\begin{aligned} T_y = {} & \frac{3\mu K_0 r_0^3 m_2}{R^3}\theta\sin\psi\left[-\cos\left(\varphi+\psi\right)\cos 2\left(\varphi+\psi-4\zeta\right) - \sin\left(\varphi+\psi\right)\sin 2\left(\varphi+\psi-4\zeta\right)\right] - \\ & \frac{\mu K_0 r_0^3 m_2}{R^3}\theta\sin\psi\cos 3\left(\varphi+\psi-4\zeta\right) \end{aligned} \quad , \tag{2.22b}$$

and we recall that T_z is not a quantity of interest.

This completes the determination of the forces and torques arising from both the load and the trapping configurations, and hence of the linearized equation of motion of the system.

3 Analysis of system dynamics

This is of course the Section where there are actual conclusions. The first Subsection simplifies the equations of motion (2.15, 2.16, 2.21, 2.22) by doing some frequency scale separations, and then does a stability analysis. The next Subsection compares the predictions of the theory with simulation results. The Article then ends with a brief coda.

3.1 Time scale separation and stability analysis

The equations of motion I obtained above feature several contrasting time scales. Equation (2.15) has dc terms along with $2\dot{\psi}$ and $4\dot{\psi}$ (in general, spin will be much faster than precession). Equation (2.21) brings $2\left(\dot{\psi}-4\dot{\zeta}\right)$. The torque equations also have multiple time scales. A rigorous stability analysis of such a system will be extremely difficult due to the presence of all these scales – even the starting point of such a calculation (multiple order direct partition of motion? some direction partition combined with some kind of slow flow?) is not a priori apparent. For now at least, I will bypass this process but instead give somewhat general arguments which motivate the stability rather than calculating it exactly. Equation (2.15) has the obvious component

$$M\ddot{z}_{CM} = -2C_2 m_1 z_{CM} \quad , \tag{3.1}$$

which indicates outright stability in z. In the perpendicular direction there are the terms (after averaging over fast scales)

$$M\begin{bmatrix} \ddot{x}_{CM} \\ \ddot{y}_{CM} \end{bmatrix} = \begin{bmatrix} \dfrac{C_1 m_2}{r_0} + C_2 m_1 & 0 \\ 0 & \dfrac{C_1 m_2}{r_0} + C_2 m_1 \end{bmatrix} \begin{bmatrix} x_{CM} \\ y_{CM} \end{bmatrix} \quad , \tag{3.2}$$

which obviously constitute a repeller. The m_1 terms here are required by Earnshaw's theorem; the m_2 terms can be reversed to oscillator if we flip their signs. Equation (2.21),

$$M\begin{bmatrix} \ddot{x}_{CM} \\ \ddot{y}_{CM} \end{bmatrix} = \frac{6\mu K_0 r_0 m_2}{R^3} \begin{bmatrix} -\cos 2\left(\varphi+\psi-4\zeta\right) & \sin 2\left(\varphi+\psi-4\zeta\right) \\ \sin 2\left(\varphi+\psi-4\zeta\right) & \cos 2\left(\varphi+\psi-4\zeta\right) \end{bmatrix} \begin{bmatrix} x_{CM} \\ y_{CM} \end{bmatrix} \quad , \tag{3.3}$$

is the Brouwer saddle. Although the analysis (1.2) is over-simplified (it does not agree very well with simulation), there are clear cut regions in the strength vs. frequency parameter space where the system is stable at the slow level. A sufficiently strong Brouwer saddle will counteract the repeller terms in (3.2).

To process the torque equations, we must convert from x,y,z to a,b,c basis since (2.4) is written in that basis. At the linear level, a,b,c is just x,y,z rotated through φ about z. Before conversion however, we must recognize that there are two classes of terms in (2.16) and (2.22). One class is where the torque is developed about some fixed axis, while the second class is where it is developed about the axis along which the rotor has nuted. Terms of the former type are best left as is, while those of the latter are brought over to a,b,c basis. After this step, we extract dc quantities from the torque equations by averaging over ψ and other fast scales. This yields, on a dc level for the nutation axis,

$$T_a = \theta\left(4m_1 B_0 - 3C_1 m_2 r_0\right) \quad , \tag{3.4a}$$

$$T_b = 0 \quad . \tag{3.4b}$$

The first term in T_a is the tendency of the load dipoles to align with 'magnetic North' of the load field. The second term contains the effect of whether the trapping dipoles point inwards or outwards; inwards (as here) tends to oppose nutation while outwards supports it. The vanishing of T_b is also physically plausible – a small nutation should induce an average torque about the nuting axis and not a perpendicular axis.

We also have the ostensibly dc terms about a fixed axis

$$T_x = \left(2C_1 m_1 - C_2 m_2 r_0\right) y_{CM} \quad , \tag{3.5a}$$

$$T_y = -\left(2C_1 m_1 - C_2 m_2 r_0\right) x_{CM} \quad . \tag{3.5b}$$

Finally, averaging of (222) yields an oscillating term of the form

$$T_a = \theta\left[\frac{3\mu K_0 r_0^3 m_2}{2R^3}\cos 4\zeta\right] \quad . \tag{3.6}$$

Here is the term which needed the trapping field to be rotated relative to the laboratory. It is directed along the axis of nutation because that is where the torque is strongest and oscillates at $4\dot{\zeta}$ because the trapping field is rotating at that rate past the nutational axis.

The treatment of (3.4) is standard : assuming fast spin in (2.4a), there is a fixed point where the precession frequency $\Omega^* = T_a / I_c \dot{\psi}\theta$, and this fixed point is stable to perturbations. However, there are the extra torques (3.5, 3.6) : how do we handle those ? Equation (3.6) describes an oscillatory torque, while (3.5) seems to imply a constant torque; in the presence of such a torque the uniformly precessing fixed point no longer exists.

The way out of this trap is to recognize that x_{CM} and y_{CM} are themselves oscillatory on account of the Brouwer saddle. Thus, if there is an initial perturbation in y_{CM}, that variable will continue to oscillate at the effective spring frequency, and T_x will also become an oscillatory term. We now determine the stability of the rotation in the presence of an oscillatory torque. In the limit of fast spin, the rotor angular momentum vector **L** points along its axis. As the rotor precesses, the tip of this vector traces out a circle in the horizontal plane. The radius of the circle is the horizontal component of **L** i.e. $L\sin\theta^*$ or $L\theta^*$ where θ^* is the equilibrium nutation angle. In the absence of the oscillatory torque, the value of θ^* is not unique; any value suffices for a balance between the applied torque and the precession. Now in the presence of oscillatory term, we claim that there is a unique value of θ^* and a unique trajectory followed by the tip of the **L** vector. For conceptual and mathematical simplicity, I will replace the sinusoidal torque about the x-axis by a series of alternating kicks. I will assume that for one half-period the external torque is quiet, and then there is an impulse in the $+x$-direction; then after another half-period of quiescence, there is another impulse in the $-x$-direction. Under such an excitation, the tip of **L** will trace out a circle for a half-period, then jump over to a new value, again trace out a circle and then jump back etc. For the proper value of θ^*, the trajectory will close on itself. This closed orbit is shown in Fig. 3.

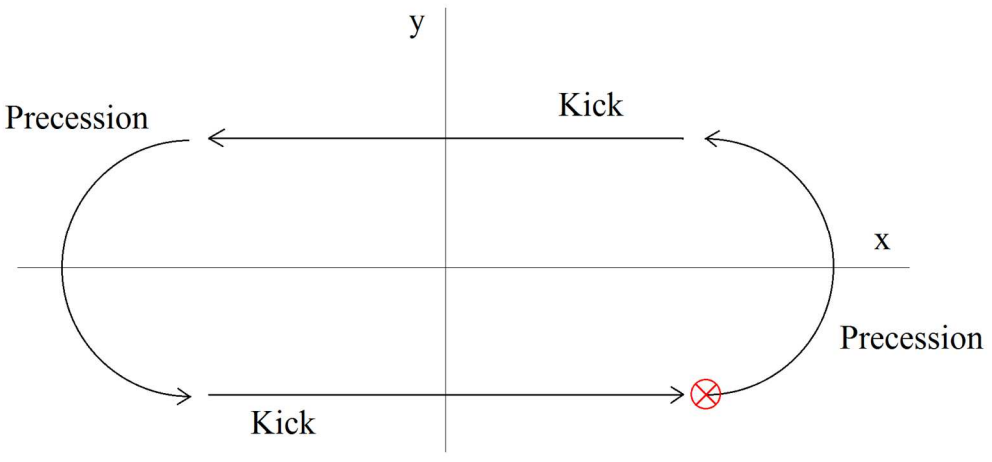

Figure 3 : *Orbit traced by the tip of **L** during precessional motion in the presence of an oscillatory torque. The red point is the "starting point" of the trajectory, for the purposes of the analysis which follows.*

If the magnitude of each kick be τ and the half-period be $1/\mu$, then in Fig. 3, the top right corner of the trajectory has the coordinates $L\theta^*\left(\cos(\pi\Omega^*/2\mu), \sin(\pi\Omega^*/2\mu)\right)$. By symmetry, the abscissa of the top left corner must be the negative of that; since the difference between the two is τ, that gives the relation

$$2L\theta^* \cos\frac{\pi\Omega^*}{2\mu} = \tau \quad , \tag{3.7}$$

i.e. θ^* gets determined in terms of τ, or in terms of the oscillatory torque.

So we have shown that an oscillatory state of the rotor exists; is it stable ? To answer this question, we will again consider the curve traced by the tip of **L**, Fig. 3. Assume that the evolution 'starts' when the tip is at the bottom right corner, which we call $[x_0; y_0]$. After precession during one half-period of the excitation, this point evolves into (letting ξ be the angle of precession) $\mathbf{Z}(\xi)[x_0; y_0]$. At that time it adds on the vector $[-\tau; 0]$, then again gets operated on by

$\mathbf{Z}(\xi)$, and then adds on $[+\tau; 0]$. At this point, if $[x_0; y_0]$ are those of the steady state trajectory, the tip comes back to where it started. We want to know what happens if $[x_0; y_0]$ is slightly shifted from the steady state value.

This is thus the question of stability of the two-variable map

$$\begin{bmatrix} x_{n+1} \\ y_{n+1} \end{bmatrix} = \mathbf{Z}(\xi)\left(\mathbf{Z}(\xi)\begin{bmatrix} x_n \\ y_n \end{bmatrix} - \begin{bmatrix} \tau \\ 0 \end{bmatrix}\right) + \begin{bmatrix} \tau \\ 0 \end{bmatrix} \quad . \tag{3.8}$$

Tacking on perturbations Δx and Δy to the steady state values x_0 and y_0, we see that they satisfy

$$\begin{bmatrix} \Delta x_{n+1} \\ \Delta y_{n+1} \end{bmatrix} = \begin{bmatrix} \cos 2\xi & -\sin 2\xi \\ \sin 2\xi & \cos 2\xi \end{bmatrix}\begin{bmatrix} \Delta x_n \\ \Delta y_n \end{bmatrix} \quad . \tag{3.9}$$

This is of course a rotation matrix so the perturbations remain bounded and the system is stable.

This analysis shows that the rotating rotor will remain stable in the presence of an oscillatory torque. All these put together strongly indicate that the proposed design of trap will have regions of stable operation. We now go on to the simulation results.

3.2 Simulation results

(This block uses the BRIAN TAIT angle convention for rotational dynamics.)

Although the natural equations of motion to simulate would have been (2.1-4), it turns out that this choice poses a big problem. Near the zero nutation limit, where we want to operate the system, the precession and spin tend to coalesce. While this coalescence is not a problem theoretically, it is a near-insurmountable hurdle for Matlab, which was taking hours to solve the system for a few tenths of a unit of real time. This block is removed by recasting the rotational dynamics in the BRIAN TAIT or aircraft angle convention. This reformulation reduces physical insight and analytical convenience (which is why the heavy symmetric top is traditionally not solved in these angles) but it facilitates the simulation enormously. The time required for a given run of the system decreased by one to two orders of magnitude after the change from the gyro convention to the aircraft convention.

Hence, starting from the x,y,z basis centred at the rotor CM, we now perform the first rotation through angle φ about the x-axis to get to x',y',z', then the next rotation through θ about y' to get to a,b,c and then the third through ψ about c to get to d,q,o. Although I have kept the angle and basis notation the same, the rotations here (except for the third one) are completely different, and the new meanings of these notations are valid only in this Subsection.

In the Tait *X-Y-Z* convention, the rotation matrices are

$$\mathbf{R}_{xyz}^{abc} = \mathbf{Y}(\theta)\mathbf{X}(\varphi) = \begin{bmatrix} \cos\theta & \sin\varphi\sin\theta & -\cos\varphi\sin\theta \\ 0 & \cos\varphi & \sin\varphi \\ \sin\theta & -\sin\varphi\cos\theta & \cos\varphi\cos\theta \end{bmatrix} \quad , \tag{3.10a}$$

$$\mathbf{R}_{xyz}^{dqo} = \mathbf{Z}(\psi)\mathbf{Y}(\theta)\mathbf{X}(\varphi) = \begin{bmatrix} \cos\theta\cos\psi & \cos\varphi\sin\psi + \sin\varphi\sin\theta\cos\psi & \sin\varphi\sin\psi - \cos\varphi\sin\theta\cos\psi \\ -\cos\theta\sin\psi & \cos\varphi\cos\psi - \sin\varphi\sin\theta\sin\psi & \sin\varphi\cos\psi + \cos\varphi\sin\theta\sin\psi \\ \sin\theta & -\sin\varphi\cos\theta & \cos\varphi\cos\theta \end{bmatrix} \quad . \tag{3.10b}$$

The locations and orientations of the dipoles relative to the d,q,o basis remain as they were in Subsection 2.1 but their x,y,z expressions change on account of the above. The rotational equations of motion are (again obtained by evaluating material derivative of $\mathbf{L}$ in a,b,c)

$$I\ddot{\varphi}\cos\theta + (I_c - 2I)\dot{\varphi}\dot{\theta}\sin\theta + I_c\dot{\theta}\dot{\psi} = T_a \quad , \tag{3.11a}$$

$$I\ddot{\theta} + (I - I_c)\dot{\varphi}^2\cos\theta\sin\theta - I_c\dot{\varphi}\dot{\psi}\cos\theta = T_b \quad , \tag{3.11b}$$

$$I_c\left(\ddot{\psi} + \ddot{\varphi}\sin\theta + \dot{\varphi}\dot{\theta}\cos\theta\right) = T_c \quad . \tag{3.11c}$$

The simulation now proceeds as follows :

- The computer calculates the load field by integrating (2.5).
- The computer calculates the trapping field using the formula (2.18-19).

- The computer calculates the positions and orientations of all the dipoles using (3.10).
- The computer calculates the forces and torques using (2.2). Gradient of **B** is evaluated numerically.
- The computer converts **T** from x,y,z to a,b,c basis using (3.10).
- Finally the computer numerically integrates the twelfth order system (2.3) and (3.11) using a stiff solver.

Although I generally prefer to use SI units for simulations, I have made an exception here so that r_0 could be made of size 1. Hence, all the simulation results are in terms of arbitrary units rather than SI. The numerical values assigned to various quantities for the upcoming runs are summarized below :

- Load coils
  - Inner coil radius 1.00
  - Outer coil radius 1.10
  - $\mu i/4\pi$ set equal to 1
- Trapping coils
  - Polarity 8
  - $\mu K_0/2R^3$ set equal to 16000
  - Spin rate variable
- Rotor
  - Radius 1.05
  - Mass 1000
  - Acceleration due to gravity 10
  - Axial moment of inertia 5000
  - Transverse moment of inertia 2500
  - Number of load dipoles 4
  - Strength of load dipoles 10
  - Number of trapping dipoles 2
  - Strength of trapping dipoles 10

For the load coils I found that at ρ=1.05, the maximum F_z occurs at z=about 0.05 and its value is about 40000. As the default operating point here, I have chosen z_0=0.1, where F_z decreases to about 10000. This ensures plenty of cushion between the cruising altitude and the critical altitude, beyond which the rotor loses static stability in z. The moment of inertia is quite large compared to the mass and the radius; I have implicitly assumed while selecting these values that the dipoles are mounted at a smaller radius (by a factor of about 3) than the full radius of the rotor. Since large moment of inertia is beneficial, that is a natural place to mount them. The value of 16000 for the strength of the trapping field is based on some preliminary simulations of maximum stability of a Brouwer saddle; it generates a force equal to the rotor weight at a displacement of 0.005 unit. The corresponding rotation frequency $\dot{\psi} - 4\dot{\zeta}$ is about 50.

To facilitate convergence of the simulations, I have introduced first order damping in all the equations (2.3) and (3.11) except for (3.11c). This damping is proportional to the velocity or angular velocity by a factor whose value is 1 for the translational modes and 0.4 for the rotational ones. We note that such damping cannot overturn the effect of a repelling potential; $\ddot{x} + \gamma\dot{x} - x = 0$ is always unstable, however large γ may be. The physical explanation for this is that the particle becomes slow enough that the damping force is insignificant and then crawls out along the potential. Rather, a light damping converts the 'borderline' stability of an oscillator potential, which is the type we saw in Subsection 3.1 and is generally the only type found in a non-dissipative system, into absolute stability. This makes the simulation runs and their conclusions more reliable. Finally, to accelerate the simulation speed, I have replaced the actual, rapidly fluctuating T_c with its average value of zero.

In Fig. 4, I plot the time traces, upto a time of 10 units, of all the position and orientation variables with $\dot{\zeta} = 4$ and $\dot{\psi} = 63$. The initial condition is x_{CM}=0.03, φ=0.003 and all other perturbations are zero. The stability of motion is apparent from this Figure.

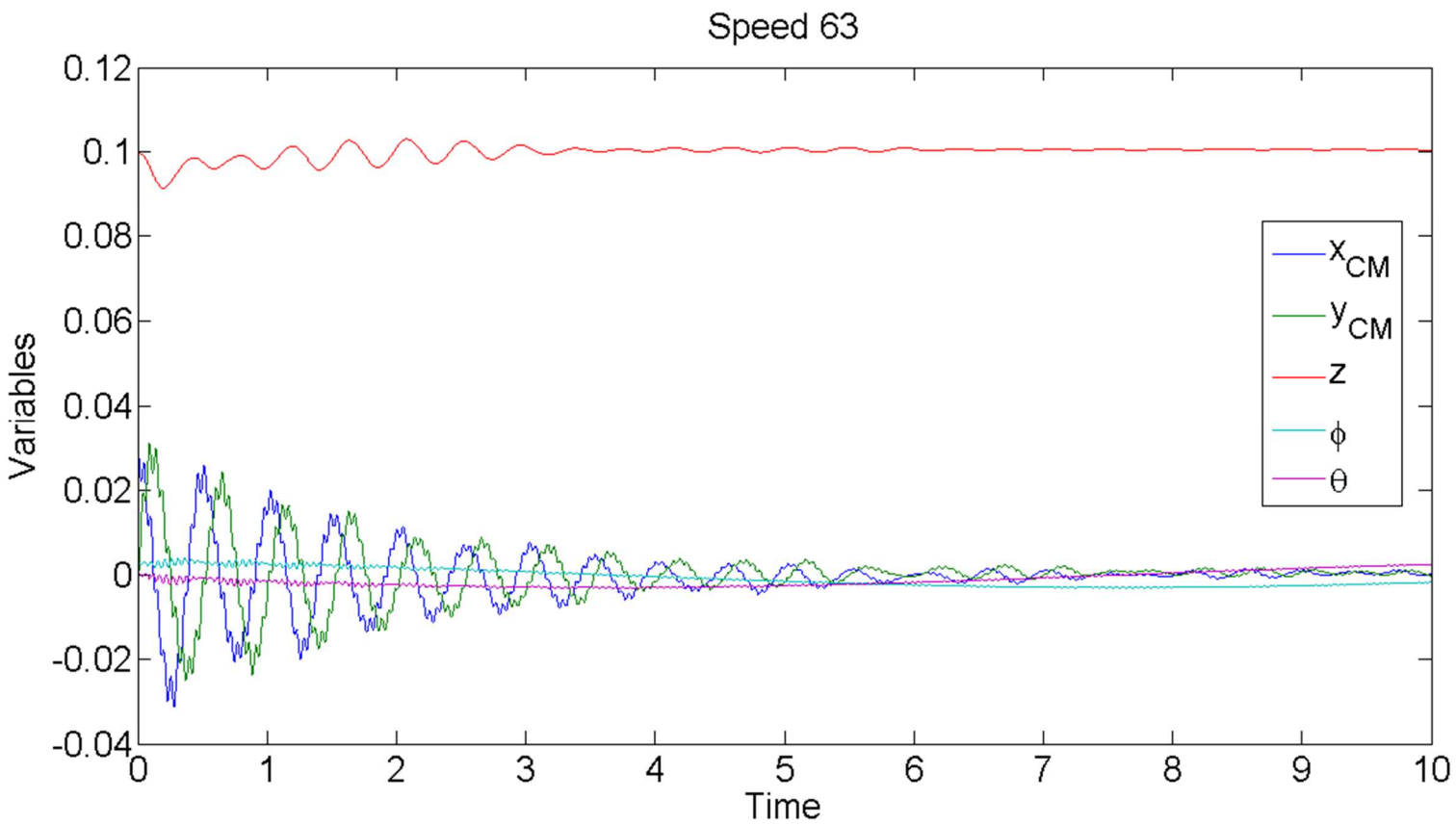

Figure 4 : *Simulation run of the system. We can see that the initial translational and rotational perturbations die down, implying that confinement of the rotor has been achieved.*

In another simulation run, we try a rotation speed of 110. The field rotation rate is 15, so that four times that is 50 less than the rotor speed. The initial condition is that x_{CM}=0.02 and everything else same as in Fig. 4. The results are in Fig. 5.

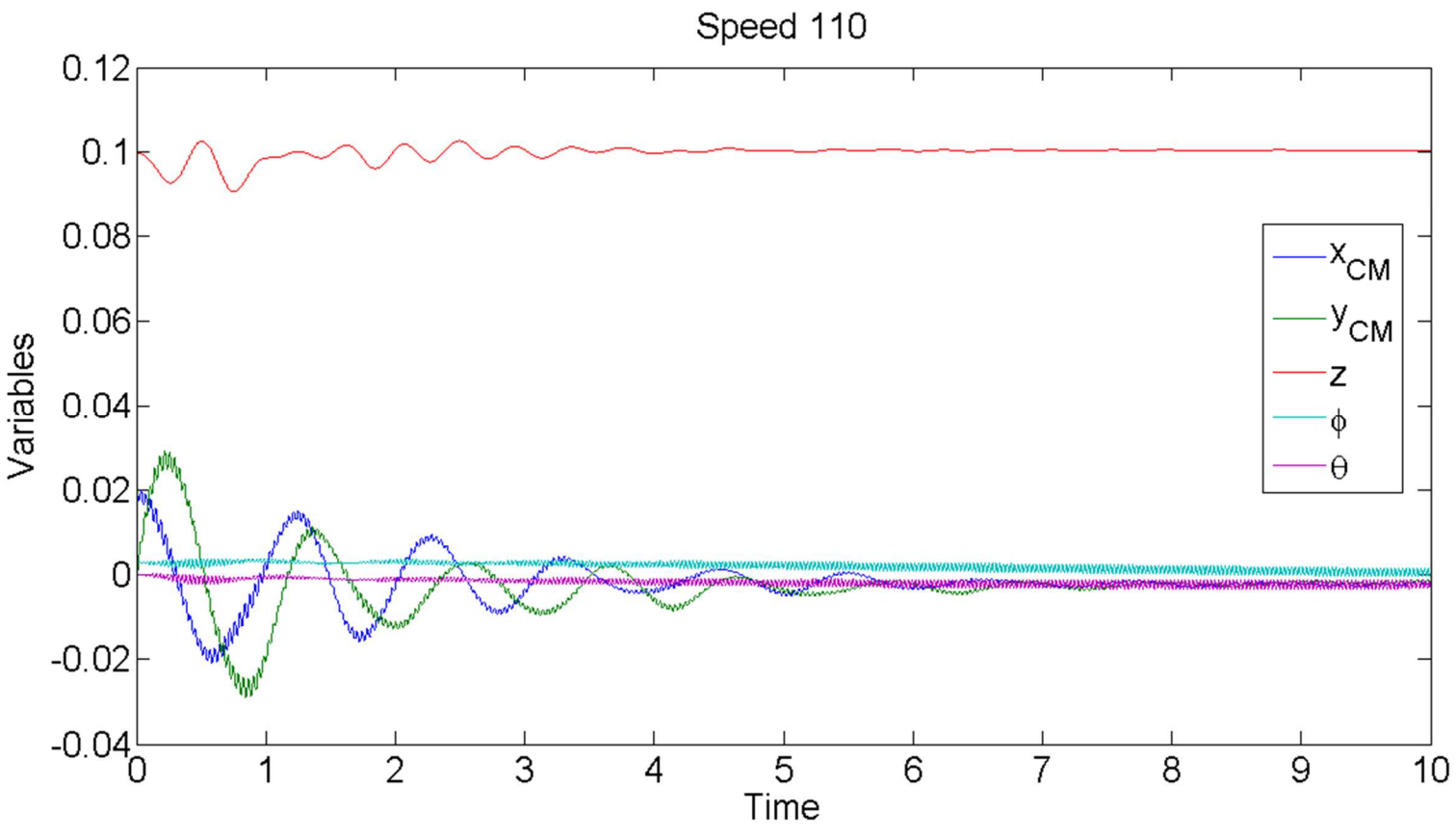

Figure 5 : *Simulation run of the system at nearly double the speed of Fig. 4. Once again we observe the decay of the perturbations in time.*

The simulations indicate convincingly that the proposed trap is effective.

3.3 Conclusion

So where are we after all this ? My aim here was to propose a design for a mechanism which would achieve electromagnetic confinement of a rigid body with no position control. Moreover, I wanted an arrangement which would allow for adjustments in size and stability unlike the HHB mechanism and would be easy to manufacture and operate unlike my earlier helix. To this end, I described a design where the load coils generate weight support and z-stability and the trapping coils counteract the resultant x,y instability through the Brouwer saddle action. Physical arguments, mathematical calculation and numerical simulation all indicate that this design achieves its intended purpose.

The construction of this device is undoubtedly easy. The apparatus is compact and the fanciest component required is a three-phase winding with an inverter – something which can be found a dime a dozen in a power electronics laboratory. One big advantage of this design over the HHB mechanism is the largish number of free, tunable parameters in the system. The number and strength of load dipoles can be adjusted as per the rotor weight. The number, strength and sign of the trapping dipoles can all be varied to increase the stability. The strength and polarity of the trapping field are also variable, as is the relative rotation rate between the field and the rotor. Then of course there are infinite possibilities to play with the configuration itself – tweak the wires to increase a field here, decrease a gradient there.

The vast majority of this huge parameter space is unexplored – the simulations I have run so far constitute a set of measure zero. For these trial runs, I have used a trapping field which is thousand times stronger than the load field; for a practical design we need operating points where this ratio can be smaller. The stability analysis of the system is also unchartered territory; Subsection 3.1 convinces us that for some parameter values the trap will work, but by no means tells us where the stability boundaries lie and where the operation is most effective. As an example, we see that the oscillation frequency of x_{CM} and y_{CM} in Fig. 4 is almost double that in Fig. 5. Hence the parameter values of Fig. 4 produce a stiffer spring i.e. a more stable trap than those of Fig. 5. This is also evident from the fact that an initial perturbation of 0.03, which was contained by the trap in Fig. 4 is in fact sent off to infinity in Fig. 5. In fact, if I increase rotor speed further to 120, the stability vanishes altogether. Right now I do not have any explanation for this; perhaps some nonlinear coupling gets excited or else some kind of parametric resonance takes place.

There is also the issue of damping. In Matlab, a $-\gamma\dot{x}$ can just be thrown in by hand; in reality it will need a lot of clever thinking and experimentation. The likely source of damping will be eddy currents from a separate mechanism. Another possibility is to have a viscoelastic rotor or aerodynamic spoilers, but then we must ensure that they do not damp out the rotor spin also. The design and calculations for the damper will likely be as difficult as they were for this trap, and how to make an effective damper without making things inordinately heavy or cumbersome is a very much open question.

Yet, as much as there are questions, there are also possibilities. Despite enormous amount of research, magnetic levitators are still far from occupying the prominent position in technology which they deserve. When the superconducting bearings had become almost-reality in the 1990s, the researchers' excitement was palpable. None puts it better than FRANCIS MOON [7], "Passive, simple and defying intuition – these are the defining qualities of superconducting levitation. One can imagine the relative velocity of 100-200 m/s between moving bodies with no contact, no wear, no need for fluid or gas intervention and no need for active controls." Although that line of thought ended up in a dry channel, a new proposed technology always raises the same kind of hopes. While magnetically levitated fans, compressors and centrifuges are humdrum, a more exotic and useful application can be in flywheel energy storage devices. At large rotational speeds, these are far more energy-dense than batteries; at really high speeds they can approach fossil fuels. To sustain the speed for a long time without guzzling energy, the friction on the wheel shaft must be minuscule. What better way to do it than using magnetic levitation ? And the plus-points of alternative energy sources in today's polluted and fuel-scarce world are too obvious to even mention.

On this note, let me conclude the Article with an explicit statement of what I wish to see the most – a real trap for real rigid bodies working in a laboratory and in the field, and not just on the journal pages. I hope that we all can work towards making this dream a reality.

* * * * *

Miscellanea

Certificate of honest simulation : I have made every possible effort to ensure that the simulations performed here are a faithful model of the actual system. If there still are any errors in the code resulting in alterations to the conclusions of Subsection 3.2, then those are the result of an academic mistake and not academic malpractice. Any legitimate request for the code from a bonafide third party will be complied within 24 hours except under exceptional circumstances.

Data accessibility : This Article does not report or rely on any experimental data.

Competing interests : There are no competing interests to report for this research.

Author contribution : This work is entirely my own.

Funding statement : There are no funders to report for this research.

References

[1] DJ Griffiths, "*Introduction to Electrodynamics*," Third Edition, Pearson Education, Upper Saddle River, New Jersey, USA (2005)
[2] WR Smythe, "*Static and Dynamic Electricity*," Third Edition, Taylor and Francis, Milton Park, UK (1989)
[3] AK Geim, MD Simon, MI Boamfa and LO Heflinger, "Magnetic levitation at your fingertips," **Nature** 400, 323-324 (1999)
[4] MD Simon and AK Geim, "Diamagnetic levitation : flying frogs and floating magnets," **Journal of Applied Physics** 87 (9), 6200-6204 (2000)
[5] MD Simon, LO Heflinger and AK Geim, "Diamagnetically stabilized magnet levitation," **American Journal of Physics** 69 (6), 702-713 (2001)
[6] JG Bednoerz and KA Mueller, "Possible high Tc superconductivity in the Ba-La-Cu-O system," **Zeitschrift fur das Physik B** 64, 189-193 (1986)
[7] FC Moon, "*Superconducting Levitation*," Wiley Interscience, Upper Saddle River, New Jersey, USA (1994)
[8] W Paul, "Electromagnetic traps for charged and neutral particles," **Reviews of Modern Physics** 62 (3), 531-540 (1990)
[9] LS Brown, "Quantum motion in a Paul trap," **Physical Review Letters** 66 (5), 527-529 (1991)
[10] D Leibfried, R Blatt, C Monroe and D Wineland, "Quantum dynamics of single trapped ions," **Reviews of Modern Physics** 75 (1), 281-324 (2003)
[11] HG Dehmelt, "Experiments with an isolated subatomic particle at rest," ***ibid.*** 62 (3), 525-530 (1990)
[12] LS Brown and G Gabrielse, "Geonium theory : physics of a single electron or ion in a Penning trap," ***ibid.*** 58 (1), 233-311 (1986)
[13] G Schweitzer and EH Maslen (editors), "*Magnetic Bearings : Theory, Design and Application to Rotating Machinery*," Springer Verlag, Heidelberg, Germany (2009)
[14] MV Berry, "The Levitron : an adiabatic trap for spins," **Proceedings of the Royal Society A** 452, 1207-1220 (1996)
[15] MD Simon, LO Heflinger and SL Ridgway, "Spin stabilized magnetic levitation," **American Journal of Physics** 65 (4), 286-293 (1997)
[16] TB Jones, M Washizu and R Gans, "Simple theory for the Levitron," **Journal of Applied Physics** 82 (2), 883-888 (1997)
[17] MV Berry and AK Geim, "Of Flying frogs and Levitrons," **European Journal of Physics** 18 (4), 307-313 (1997)
[18] R Krishnan, "*Electric Motor Drives – Modeling, Analysis and Control*," Phi Learning Private Limited, Dilli (2010)
[19] H Freudenthal (editor), "*The Collected Works of LEJ Brouwer*," North Holland Publishers, Amsterdam, The Netherlands (1975) (article title : "The Motion of a particle at the bottom of a rotating vessel under the influence of the gravitational force")
[20] ON Kirillov, "Brouwer's problem on a heavy particle in a rotating vessel : wave propagation, ion traps and rotor dynamics," **Physics Letters A** 375 (15), 1653-1660 (2011)
[21] ON Kirillov and M Levi, "Rotating saddle trap as Foucault's pendulum," **American Journal of Physics** 84 (1), 26-31 (2016)
[22] RI Thompson, TJ Harmon and MG Ball, "The Rotating saddle trap : a mechanical analogy to RF electric quadrupole ion trapping?" **Canadian Journal of Physics** 80 (12), 1433-1448 (2002)
[23] T Hasegawa, MJ Jensen and JJ Bollinger, "Stability of a Penning trap with a quadrupole rotating electric field," **Physical Review A** 71, 023406 (2005)
[24] J Nilsson, "Trapping massless Dirac particles in a rotating saddle," **Physical Review Letters** 111, 100403 (2013)
[25] B Shayak, "A Mechanism for electromagnetic trapping of massive extended objects," submitted, available at www.shayak.in/Shayakpapers/Maglev/RingTrapLetter.pdf